Astron. Astrophys. 333, 17–26 (1998)

ASTRONOMY AND ASTROPHYSICS

Is the shape of the luminosity profile of dwarf elliptical galaxies an useful distance indicator?

Bruno Binggeli[1] **and Helmut Jerjen**[2]

[1] Astronomisches Institut, Universität Basel, Venusstrasse 7, CH-4102 Binningen, Switzerland
[2] Mount Stromlo and Siding Spring Observatories, Private Bag, Weston Creek PO, ACT 2611, Canberra, Australia

Received 3 April 1997 / Accepted 1 December 1997

Abstract. The shape of the surface brightness profile of dE galaxies, quantified by parameter n of Sérsic's generalized profile law, has recently been put forward as new extragalactic distance indicator (Young & Currie 1994). Its application to the Virgo cluster has subsequently led to the claim that the Virgo dEs are not lying in the cluster core but are distributed in a prolate structure stretching from 8 to 20 Mpc distance (Young & Currie 1995).

This claim is refuted here. We have fitted a Sérsic law to the surface brightness profiles of 128 Virgo cluster dEs and dS0s from the photometry of Binggeli & Cameron (1991). The dispersion of the $n - M$ relation is indeed large ($\sigma_{\rm rms} \approx 0.9$ mag). However, we argue that this scatter is not due to the depth of the Virgo cluster, but is essentially intrinsic. Contrary to what one would expect from the cluster depth hypothesis, there is no clear velocity-"distance" relation for a sample of 43 Virgo dEs and dS0s with known redshifts. The analysis of Young & Currie (1995) is hampered by the use of low-resolution photometry and flawed by the assumption that the $n - M$ and $n - R$ relations can be used *independently*.

By combining different Sérsic law parameters, the scatter of the scaling relations can be reduced somewhat, but never below $\sigma_{\rm rms} \approx 0.7$ mag, at least for the Virgo cluster. For the purpose of distance measurements, this falls short of the well-established Tully-Fisher and $D_{\rm n} - \sigma$ methods, and it is comparable to what one can get already from the $\langle\mu\rangle_{\rm eff} - M$ relation for dEs, which does not require any profile modelling.

Key words: galaxies: distances and redshifts – galaxies: elliptical and lenticular, cD – galaxies: fundamental parameters – galaxies: photometry

1. Introduction

The surface brightness profile of dwarf elliptical (dE) galaxies follows a 3-fold trend: with increasing galaxy luminosity (1) the mean surface brightness increases, (2) the profile becomes flatter in the outer region, while (3) the profile becomes more cuspy, i.e. more E-like in the core region (Binggeli & Cameron 1991). The two latter characteristics, combined in the overall *shape*, or *curvature* of the dE profile, can be quantified and parametrized by means of Sérsic's (1968) r^n law for the radial surface brightness profile of galaxies, which is a simple generalization of de Vaucouleurs' $r^{1/4}$ and exponential laws (Davies et al. 1988, Young & Currie 1994, Jerjen 1995). The profile curvature of dEs is described by Sérsic's exponent n.

Working with a small sample of Fornax cluster dEs, Young & Currie (1994, hereafter YC94) found that the correlation between n and total magnitude of the galaxy was so tight, with an rms scatter of only ≈ 0.47 mag, that it could be used to derive a distance of the Fornax cluster, based on a handful of local, calibrating dEs. Hence the claim of a "new extragalactic distance indicator".

In a second paper, Young & Currie (1995, hereafter YC95) applied a variant of this new distance indicator, viz. the relation between n and the logarithm of Sérsic's scale length r_0 (see below), to a sample of 64 Virgo cluster dEs, for which they had derived profiles from low-resolution Schmidt plates. The scatter of the $n - \log r_0$ relation turned out to be much larger for these Virgo cluster dEs than for an external sample of Local Group and Fornax cluster dwarfs. Nevertheless, YC95 argued, by way of comparing the results from the apparently independent $n - M$ and $n - \log r_0$ relations, that the *intrinsic* scatter for Virgo cluster dEs would be equally small. The inevitable conclusion on this assumption was that the large observed scatter for Virgo cluster dEs must be attributed to the *depth* of the Virgo cluster. Moreover, the resulting filamentary cloud of dEs, stretching from ca. 8 to 20 Mpc in Young and Currie's distance scale, and apparently by chance (?) being aligned with our line of sight, is in perfect accord with the filament of spiral galaxies advocated by Fukugita et al. (1993) and Yasuda et al. (1997) based on Tully-Fisher distances.

This we found alarming. Spiral galaxies are supposed to avoid the core of the Virgo cluster (Binggeli et al. 1987). However, from all we know (cf. Ferguson & Binggeli 1994 for a recent review, Stein et al. 1997) – dwarf ellipticals, like ellipticals in general, reside only in dense galaxy environments, which would exclude loosely bound clouds or filaments of galaxies.

Send offprint requests to: B. Binggeli (binggeli@astro.unibas.ch)

Motivated by this contradiction, we went back to the Virgo cluster photometry of Binggeli & Cameron (1991, 1993, hereafter BC91 and BC93) and selected 128 highly resolved dE and dS0 profiles that are well explained by Sérsic's generalized law. This sample, as well as the procedure and the results of the fitting are presented in Sect. 2. Our analysis of the data, in Sect. 3, confirms that the scatter of either the $n - M$ or the $n - \log r_0$ relation is very large. It cannot be reduced to below ca. 0.7 mag, which is comparable to the scatter of the surface brightness - luminosity ($\langle\mu\rangle_{\rm eff} - M$) relation (BC91). This is simply too large for a distance indicator to be useful – *if* the scatter is intrinsic.

As we argue in Sect. 4, there is indeed some evidence that this large scatter for Virgo *is* intrinsic, i.e. cosmic. The residuals from the $n - M$ and $n - \log r_0$ relations do not correlate with the velocities of the dwarfs – which they should if these galaxies were distributed in a filament outside the Virgo cluster core. We also discuss why we think Young & Currie's analysis is flawed. Our sober conclusions are given in Sect. 5.

2. Generalized profile parameters of Virgo cluster dwarfs

Following the notation of YC94, Sérsic's (1968) generalized profile law can be written as

$$\sigma(r) = \sigma_0\, e^{-(r/r_0)^n} \ , \tag{1}$$

where σ is the surface brightness (light intensity per area) at the mean galactocentric radius r. There are three parameters: (1) the central surface brightness σ_0, (2) the characteristic radius, or scale length r_0 at which $\sigma = \sigma_0/e$, and (3) the shape parameter n. The corresponding law in the magnitude (logarithmic) representation is

$$\begin{aligned}\mu(r) &= -2.5\log\sigma(r) + const \\ &= \mu_0 + 1.086\,(r/r_0)^n \ ,\end{aligned} \tag{2}$$

with $\mu_0 = -2.5\log\sigma_0 + const$. The quantity μ is again called "surface brightness" but has now the conventional unit of (mag arcsec^{-2}). For $n = 1$ Sérsic's law is identical to the exponential; for $n = 1/4$ it reduces to de Vaucouleurs' (1948) $r^{1/4}$ law. In fact, Sérsic (1968) expressed his law in terms of de Vaucouleurs' parameters ($\mu_{\rm eff}, r_{\rm eff}$), which can easily be transformed to (μ_0, r_0) by generalizing de Vaucouleurs' exponent 1/4 to 1/n; hence $n_{\rm Sérsic} = 1/n_{\rm here}$.

It has become clear in recent years that Sérsic's (1968) generalization of de Vaucouleurs' law is fully explaining the variety of luminosity profiles of normal elliptical galaxies (Caon et al. 1993, D'Onofrio et al. 1994). As we now realize, it also provides an excellent description of the profiles of *dwarf* ellipticals. Unfortunately, BC91 were not aware of this law (in spite of Davis et al. 1988) but fitted exponentials and King (1966) models to their large ($N \approx 200$) and homogeneous set of well-resolved light profiles of early-type Virgo dwarfs. Indeed, the exponential and King model fits were not satisfactory for bright dwarfs. There was always what was called an "extended, central luminosity excess". Sérsic's law nicely takes care of these excesses, i.e. with a Sérsic law fit there is no excess left over – except that caused by an unresolved, quasi-stellar central nucleus, if present. Furthermore, the central light deficiency observed for dwarfs fainter than $M_{B_T} \lesssim -16$ is best approximated with Sérsic's parameter n being > 1.

For the present investigation we have fitted Sérsic laws to the (unpublished) dwarf profiles of BC91/93. In contrast to YC94, who modelled their *differential* profiles with Eq. (2) by linear regression, we fitted our *growth curves* (cumulative intensity profiles) by a $\chi^2_{\rm min}$ method with the corresponding cumulative Sérsic law, which is (Jerjen 1995):

$$\begin{aligned}I(r) &= \int_0^r \sigma(R)\, 2\pi R\, dR \\ &= \frac{2\pi\sigma_0 r_0^2}{n}\cdot\gamma[2/n, (r/r_0)^n] \ ,\end{aligned} \tag{3}$$

where $\gamma[a,x] = \int_0^x exp(-t)\, t^{a-1} dt$ is the Incomplete Gamma function. The *total* model intensity is then:

$$I_{\rm T} = I(\infty) = \frac{2\pi\sigma_0 r_0^2}{n}\cdot\Gamma[2/n] \ , \tag{4}$$

with Γ as the well-known Gamma function, or – in terms of magnitudes –

$$m_{\rm T} = \mu_0 - 5\log r_0 + 2.5\log(n/\Gamma[2/n]) - 2.00 \ , \tag{5}$$

which can be compared with the corresponding *measured* $B_{\rm T}$ value to test the goodness of a fit.

The innermost 3″ of the galaxy profiles were excluded from the fitting in order to avoid the central, semi-stellar nuclei of the dwarfs classified dE,N (or dS0,N). Likewise, an outer limiting radius for the fitting was set at a surface brightness level of 27.0 B arcsec^{-2}.

Our sample drawn form BC93 was restricted to dwarfs brighter than $B_{\rm T}^{\rm lim}$ = 18, which had also been the limit of completeness for the surveyed cluster region (cf. BC91). This left 158 objects. Ten of these were excluded because their modelled total magnitude, calculated with Eq. (5), differed from the measured $B_{\rm T}$ by more than 1 mag, the reason for the discrepancy being due to the presence of a very strong central nucleus or some irregularity in the outer profile. Aside from these cases, the mean and standard deviation of the difference between model and observed total magnitude is (model *minus* observed) 0.05 $\pm$ 0.26, which clearly shows the goodness and appropriateness of the Sérsic law.

Although we think that the growth curve fitting is more reliable than the differential profile fitting, we have performed the latter as well, as a test for consistency. Mean and standard deviation of the difference in the Sérsic parameters, determined in both ways (growth curve *minus* differential), amount to $\Delta n = -0.003 \pm 0.16$, $\Delta(\log r_0) = -0.04 \pm 0.40$ (r in arcsec), and $\Delta\mu_0 = -0.09 \pm 0.59$ B arcsec^{-2}. Clearly, n is the most stable parameter of the Sérsic law. The scatter in $\Delta(\log r_0)$, however, is surprisingly large, the implications of which will be discussed further below.

For a further purification of our sample – while keeping it representative and fairly complete – , we have excluded 20 dwarfs with $|\Delta n|$ (growth curve $-$ differential) > 0.5, leaving

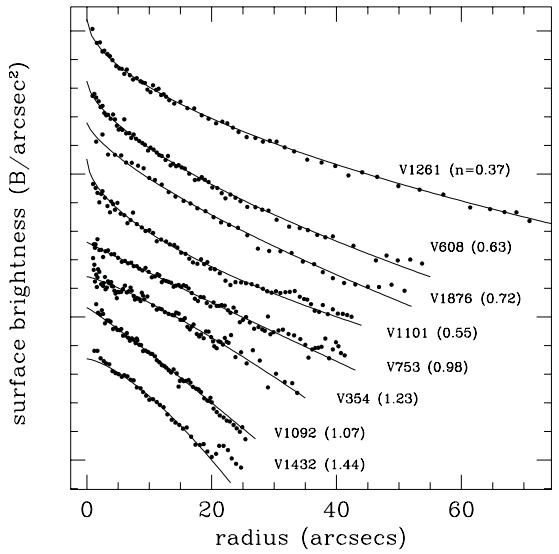

Fig. 1. Mean radial surface brightness profiles of 8 representative Virgo cluster dEs. The profiles are ordered by total magnitude (brightest object on top) but are shifted by arbitrary amounts along the ordinate. The observed profiles are given by the dots. The lines are best-fitting Sérsic profiles whose shape parameter n is given in parentheses behind the name of the galaxy. Note the systematic trend of the curvature n.

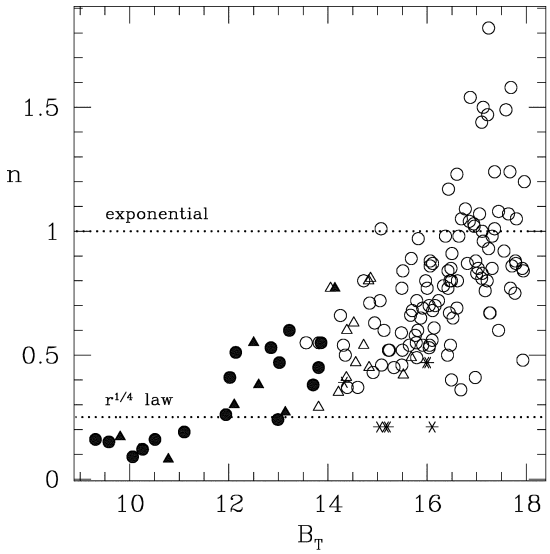

Fig. 2. Sérsic's shape parameter n versus total blue magnitude for early-type galaxies in the Virgo cluster. Dwarf galaxies (open circles: dE, open triangles: dS0) are from the present work. Data for Es (filled circles) and S0s (filled triangles) are taken from Caon et al. (1993). A few compact, M32-type Es from BC93 are added as asterisks. Note the continuity of n as opposed to the traditional bimodality (exponential versus $r^{1/4}$ law), which is indicated by the dotted lines.

us with a final sample of 128 objects. The best-fitting (growth curve) Sérsic law parameters (μ_0, $\log r_0$, n) of these 128 dwarfs are listed along with Virgo Cluster Catalog number (VCC, Binggeli et al. 1985), morphological type, total B magnitude, and heliocentric velocity (if available) in Table 1. Fig. 1 shows a few representative dwarf profiles and the corresponding Sérsic law fits.

The accuracy of the best-fitting parameters is most reliably evaluated by a comparison with external data. Unfortunately, a detailed, galaxy-to-galaxy comparison with YC95 is not useful for this purpose. Due to the low resolution of Schmidt plates, the radial profiles of YC95 are flattened, i.e. smoothed out compared with ours. Indeed, for the 30 galaxies in common we find $n_{\rm YC} - n_{\rm here} \approx 1.3 \pm 0.25 (1\,\sigma)$. Durrell (1997), whose results were published during this writing, provides high-quality data for 13 Virgo dEs, seven of which are in common with the present sample. A comparison of our Sérsic law parameters yields an rms (1σ) scatter, i.e. assumed error, for either Durrell (1997) or the present analysis, of 0.10 in n, 0.55 B arcsec^{-2} in μ_0, and 0.32 in $\log r_0$ (r in arcsec). Thus the agreement is excellent for the shape parameter n, which indeed seems to be the most robust and reliable profile parameter. On the other hand, the scatter in $\log r_0$ is again quite large. Surprisingly, it does not get smaller if we use differential profile fits (as did Durrell) – but here, part of the problem might be the presence of colour gradients in the dwarf profiles, as Durrell's (1997) data are, essentially, in the R band, ours in B.

Fig. 2 shows the $n - B_{\rm T}$ relation for our dwarf sample, complemented by Caon et al.'s (1993) data for normal ("giant") E and S0 galaxies, which we have restricted to their "good" and "fair" quality fits, and by a few compact, M32-type ellipticals from BC93, for which we have derived Sérsic law parameters in the same way as for the dwarfs. The *absolute* magnitude scale is $M_{\rm B_T} = B_{\rm T} - 31.5$, assuming $D_{\rm Virgo}$ = 20 Mpc.

Two important points are evident from Fig. 2. (1) There is indeed a clear $n - M$ relation for dwarf ellipticals which *might* be used as distance indicator. This is the topic of the present paper. (2) There is a *continuity* in the profile shape between normal and dwarf ellipticals (and S0s), with the exception of the compact, M32-type Es. In fact, this continuity holds for all three Sérsic profile parameters, not just for n (Jerjen & Binggeli 1997). This is quite surprising, because until recently the emphasis was rather on the *dis*continuity between Es and dEs in the core parameters (e.g., BC91). As it appears now, that discontinuity is restricted to the very central part of the galaxies (with galactocentric radius $r < 3''$, i.e. $r < 300$ pc if $D_{\rm Virgo}$ = 20 Mpc). The overall similarity of their light distribution strongly suggests a common formation mechanism for normal and dwarf ellipticals (but probably excluding dwarf spheroidals). For a further discussion of this aspect, the reader is referred to Jerjen & Binggeli (1997).

3. Correlation analysis

In the following we explore the correlations of Sérsic's profile parameters with total magnitude for our sample of 128 Virgo dEs and dS0s, focussing on possible applications to distance measurements. As seen in Fig. 2, the $n - M$ relation is not linear at faint magnitudes. We therefore propose to use $\log n$ instead of n. Fig. 3 shows that the $\log n - M$ relation indeed appears to be linear, i.e. is compatible with the assumption of linearity. In this

Table 1. Sérsic profile parameters of 128 Virgo cluster dEs and dS0s

VCC	Type	B_T	n	$\log r_0$ ($''$)	μ_0 (B/□$''$)	V_{hel} (km/s)	VCC	Type	B_T	n	$\log r_0$ ($''$)	μ_0 (B/□$''$)	V_{hel} (km/s)
109	dE,N	16.06	0.88	0.75	22.06		1212	dE,N	16.94	1.03	1.27	25.07	
168	dE	17.10	0.81	0.63	22.57	682	1213	dE,N	16.42	0.77	0.74	22.69	
170	dS0	14.56	0.47	0.13	20.31	1493	1254	dE,N	15.51	0.84	0.77	21.77	1350
235	dE,N	16.87	1.54	1.16	24.16		1261	dE,N	13.56	0.55	0.38	19.59	1850
299	dE	17.31	0.85	0.64	22.87		1264	dE,N	17.31	0.98	0.88	23.62	
354	dE	16.60	1.23	1.06	23.59		1268	dE,N	17.24	1.82	1.30	25.30	
389	dS0,N	14.21	0.35	–0.82	17.81	1330	1308	dE,N	15.64	0.54	–0.28	19.17	1721
444	dE	17.22	1.47	1.16	24.70		1348	dE,N	15.87	0.65	0.64	21.38	1679
490	dS0,N	14.05	0.77	0.91	21.31	1293	1353	dE,N	16.61	0.80	0.42	21.27	
494	dE	16.64	0.98	0.82	23.20		1389	dE,N	15.91	0.54	0.02	20.18	
510	dE,N	15.13	0.60	0.51	21.27		1392	dS0,N	14.86	0.81	0.93	22.09	
543	dE	14.39	0.37	–0.85	18.11	861	1396	dE,N	17.21	0.80	0.89	23.95	
554	dE,N	17.11	1.00	1.00	23.95		1399	dE,N	16.49	0.40	–0.68	19.90	
594	dE	17.13	1.50	1.05	24.15		1407	dE,N	15.49	0.46	–0.28	19.29	941
608	dE,N	14.94	0.63	0.47	20.75	1803	1417	dE	15.76	0.58	0.18	21.06	
684	dE,N	16.04	0.70	0.48	21.41		1420	dE,N	16.41	0.50	–0.28	19.96	1022
753	dE,N	16.37	0.98	1.01	23.38		1432	dE	17.10	1.44	0.94	23.46	
761	dE	17.26	0.67	0.66	23.53		1444	dE,N	16.05	0.54	–0.05	20.50	
765	dE,N	16.49	0.80	0.35	20.80		1446	dE,N	16.00	0.77	0.69	22.02	
769	dE	17.24	0.93	0.59	22.43		1451	dE,N	16.47	0.54	–0.16	20.37	
779	dE,N	17.67	1.24	1.01	24.42		1491	dE,N	15.24	0.52	–0.06	19.23	1903
781	dS0,N	14.72	0.54	0.00	19.10	–254	1496	dE,N	17.92	0.85	0.52	22.88	
810	dE,N	16.95	1.02	0.77	22.73	–340	1509	dE,N	16.42	0.84	0.78	22.71	
812	dE,N	17.03	0.85	0.73	22.99		1523	dE,N	17.64	1.07	0.75	23.40	
815	dE,N	16.10	0.56	0.26	21.23	–700	1539	dE,N	15.68	0.89	0.86	22.50	1390
823	dE,N	16.06	0.86	0.68	21.78	1691	1553	dE	16.69	1.05	1.03	23.64	
856	dE,N	14.25	0.66	0.57	20.36	972	1561	dE,N	15.82	0.97	1.17	23.78	
870	dS0,N	15.52	0.42	–0.68	18.77	1277	1563	dE,N	16.11	0.87	0.89	22.95	
871	dE,N	15.79	0.72	0.71	22.22		1567	dS0,N	14.52	0.63	0.67	21.24	1440
872	dE,N	17.00	0.83	0.63	22.55		1577	dE	16.14	0.61	0.32	21.29	
896	dE,N	17.96	1.20	0.80	23.61		1622	dE	17.87	2.47	1.17	25.06	
916	dE,N	16.04	0.53	–0.27	18.83	1349	1629	dE	17.27	0.67	0.16	21.86	
926	dE	16.97	0.41	–0.44	21.07		1661	dE,N	15.97	0.80	0.88	22.75	1400
929	dE,N	13.82	0.55	0.30	19.39	910	1688	dE	17.59	1.49	0.83	23.30	
931	dE,N	16.43	1.17	1.00	23.25		1704	dE	15.79	0.49	–0.12	20.28	
933	dE,N	16.60	0.69	0.45	22.52		1711	dE,N	16.48	0.85	0.68	22.27	
936	dE,N	15.81	0.60	0.11	20.67		1717	dE	16.50	0.91	0.96	24.22	
940	dE,N	14.72	0.80	0.83	21.45	1563	1732	dE	17.77	0.75	0.59	23.22	
949	dE,N	15.48	0.59	0.47	21.49		1743	dE	15.50	0.52	–0.04	20.21	1279
951	dE,N	14.35	0.50	0.16	19.87	2066	1745	dE	17.44	0.60	0.54	23.24	
974	dE,N	16.11	0.68	0.35	21.34		1762	dE	16.46	0.80	0.48	21.47	
992	dE,N	16.81	0.87	0.73	22.62		1767	dE,N	16.45	0.67	0.53	22.19	
1039	dE	17.11	0.83	0.60	22.60		1773	dE,N	16.16	0.70	0.65	22.32	
1044	dE,N	16.98	0.88	0.59	22.25		1779	dS0	14.83	0.45	–0.29	19.02	1226
1075	dE,N	15.08	0.46	0.00	20.21	1844	1796	dE,N	16.52	0.65	0.46	22.04	
1076	dE,N	17.36	1.24	1.04	24.19		1812	dE,N	17.78	0.88	0.61	22.79	
1087	dE,N	14.31	0.54	0.30	19.98	645	1826	dE,N	15.70	0.68	0.21	19.97	2033
1092	dE,N	17.05	1.07	0.85	23.17		1828	dE,N	15.33	0.45	–0.15	19.95	1517
1093	dE,N	16.85	1.04	0.94	23.52		1857	dE	15.07	1.01	1.14	22.67	634
1095	dE,N	17.93	0.48	–0.38	21.54		1874	dE	17.68	0.77	0.75	24.06	
1099	dE,N	17.71	0.86	0.53	22.69		1876	dE,N	15.05	0.72	0.64	21.09	45
1101	dE,N	15.78	0.55	0.32	21.47		1886	dE,N	15.49	0.77	0.65	21.40	1159
1104	dE,N	15.22	0.52	0.04	19.83	1704	1895	dE	14.91	0.43	–0.39	18.70	1032
1115	dE,N	17.69	1.58	1.09	24.61		1896	dS0,N	14.82	0.80	0.76	21.13	1731
1119	dE,N	17.36	1.01	0.78	23.25		1915	dE	17.13	0.96	0.87	23.51	
1120	dE,N	17.17	0.76	0.54	22.54		1936	dS0,N	15.68	0.49	–0.34	19.36	
1122	dE,N	14.60	0.37	–0.80	17.90	436	1942	dE,N	16.77	1.09	0.91	23.15	
1149	dE	17.44	1.08	1.23	25.28		1949	dS0,N	14.38	0.60	0.55	20.79	2077
1167	dE,N	15.91	0.69	0.60	21.88		2029	dE	17.79	0.87	0.51	22.74	
1172	dE,N	16.23	0.72	0.38	21.03		2042	dE,N	14.84	0.71	0.86	21.96	
1183	dS0,N	14.37	0.41	–0.55	18.36	1387	2043	dE	17.94	0.84	0.66	23.58	
1185	dE,N	15.68	0.66	0.53	21.56	500	2045	dE,N	16.33	0.78	0.56	21.74	
1207	dE,N	17.55	0.92	0.82	23.72		2048	dS0	13.81	0.29	–1.52	16.59	1095
1209	dE	17.80	1.05	0.62	22.89		2054	dE	16.68	0.36	–0.80	20.14	

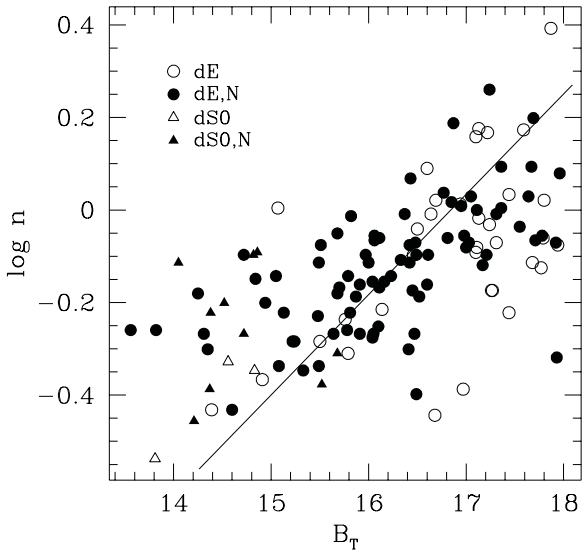

Fig. 3. The logarithm of Sérsic's profile shape parameter n versus total apparent blue magnitude $B_{\rm T}$ for 128 early-type dwarf galaxies in the Virgo cluster. Dwarf subtypes are plotted with different symbols, as given by the insert. The straight line, given by Eq. (6) in the text, is indicating the best-fitting linear correlation with $\log n$ as the independent variable.

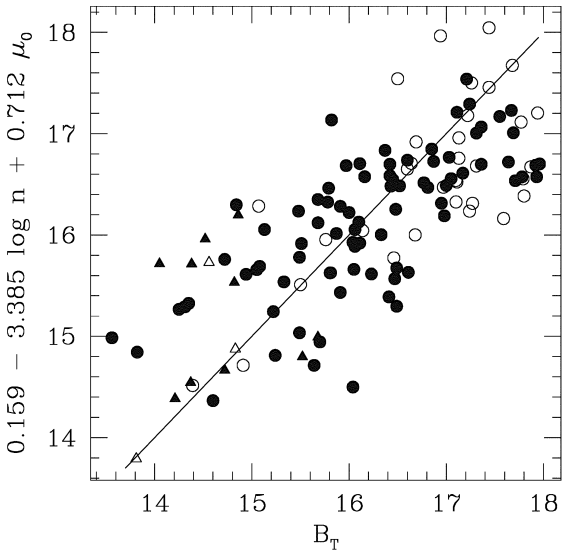

Fig. 4. The best-fitting linear combination of shape parameter n and central surface brightness μ_0, given along the ordinate [= Eq. (8) in the text], in a linear correlation with total magnitude $B_{\rm T}$. The line is identity. Sample and type coding are the same as in Fig. 3.

and the following figures we distinguish between different dwarf subtypes by plotting dE, dE,N, dS0, and dS0,N systems with different symbols. However, there is no systematic difference with respect to type, other than the well-known tendency of nucleated dwarfs to be brighter than the non-nucleated ones.

The $\log n - M$, as the $n - M$ relation for Virgo dwarfs shows a large scatter (Fig. 3), in accord with YC95. But in contrast to these authors we will attribute only a small part of this large scatter to the depth of the Virgo cluster. A linear regression for $\log n$ versus $B_{\rm T}$ gives

$$B_{\rm T} = 4.610 \log n + 16.844 \ , \qquad (6)$$

which is shown as line in Fig. 3. The fitting was restricted to objects with $\log n \leq 0$. This should approximately account for the magnitude cut-off at $B_{\rm T}$ = 18, which otherwise would artificially reduce the scatter. Note that $B_{\rm T}$ is chosen as the dependent variable because we are interested in $\log n$ as distance indicator. The rms (1σ) scatter of $B_{\rm T}$ around this line amounts to a large $\sigma_{\rm obs}$ = 0.92 mag.

Had we used differential profile fits instead of growth curve fits, the $B_{\rm T} - \log n$ relation would only slightly differ from Eq. (6), with a marginally larger $\sigma_{\rm obs}$ = 0.98, in accord with the small $\sigma(\Delta n)$ quoted in Sect. 2.

If we allow for a photometric error in $B_{\rm T}$ of $\sigma_{\rm phot} \simeq 0.2$ mag and an error of 0.08 in $\log n$ that propagates via Eq. (5) to $\sigma_{\rm profile}$ = 0.33 mag , both reckoned from a comparison with Durrell (1997), as well as a *conventional* Virgo cluster depth in terms of magnitudes of $\sigma_{\rm depth} \simeq 0.2$ mag (cf. Binggeli et al. 1987), we arrive at a still very large *intrinsic* scatter of

$$\sigma_{\rm intr} = \sqrt{\sigma^2_{\rm obs} - \sigma^2_{\rm phot} - \sigma^2_{\rm profile} - \sigma^2_{\rm depth}} = 0.81 \ {\rm mag} \ . \qquad (7)$$

Clearly, this relation is of no use for distance measurements, even if we could control, or significantly reduce the errors.

However, the correlation is significantly strengthened by plotting a linear combination of $\log n$ and central surface brightness μ_0 versus $B_{\rm T}$. The best-fitting combination, shown in Fig. 4, is

$$B_{\rm T} = -3.385 \log n + 0.712 \, \mu_0 + 0.159 \ . \qquad (8)$$

Here the fitting was restricted to objects with $\log n \leq 0$ and/or $\mu_0 \leq 24$ B arcsec^{-2}, again to avoid any bias due to the magnitude cut-off at $B_{\rm T}$ = 18. The surface brightness restriction will become plausible further below (Fig. 5). The scatter has now reduced to $\sigma_{\rm obs} = 0.73$ mag. This means that the *residuals* of the $\log n - M$ relation are correlated with μ_0. As both n and μ_0 are distance-independent quantities, their combination as given in Eq. (8) could well serve as distance indicator. But there is in fact no need to use a combination of these parameters. Surprisingly, the correlation of μ_0 *alone* with $B_{\rm T}$ is nearly as strong; see Fig. 5. The linear regression here, restricted to $\mu_0 \leq 23.5$ B arcsec^{-2}, is

$$B_{\rm T} = 0.496 \, \mu_0 + 5.426 \ , \qquad (9)$$

with a scatter of $\sigma_{\rm obs}$ = 0.76 mag. The fact that both n and μ_0 correlate with total magnitude must of course mean that n and μ_0 correlate with each other as well, which is shown in Fig. 6.

A scatter of 0.7 mag is also what one can get from the relation between the mean *effective* surface brightness $\langle\mu\rangle_{\rm eff}$ and total magnitude (BC91, Jerjen 1995). The effective surface brightness has the great advantage to be *model-independent*. So there is apparently no gain by the profile fitting *with respect to the distance indicator application*.

In their second paper, Young & Currie (YC95) propose the $n - \log r$ relation as an alternative to n versus M as distance

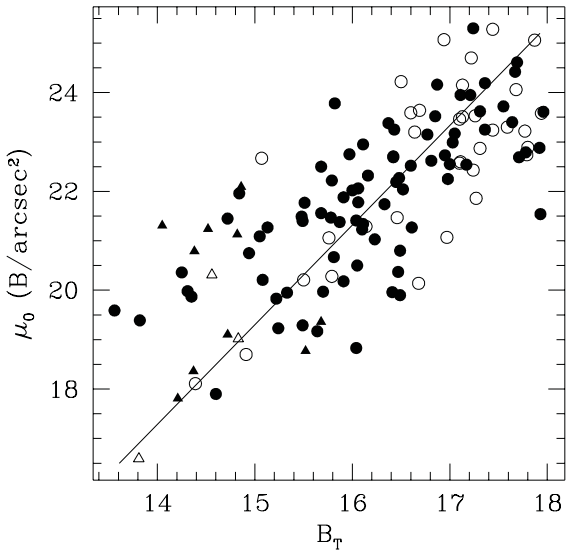

Fig. 5. Sérsic's central surface brightness μ_0 versus total magnitude $B_{\rm T}$. The linear regression line, with μ_0 as independent variable, is given by Eq. (9) in the text. Sample and type coding as in Fig. 3.

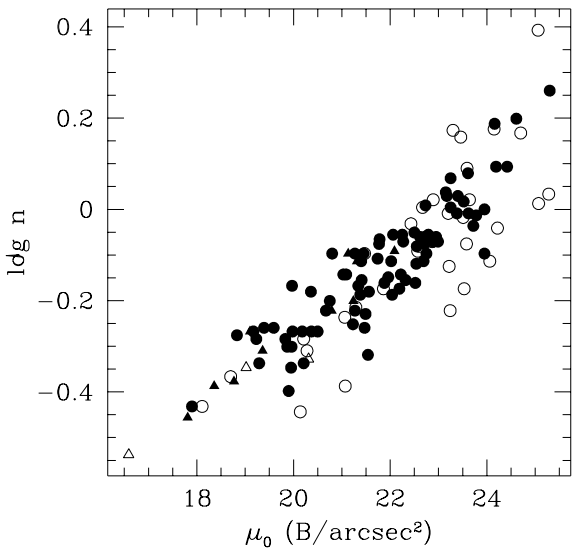

Fig. 6. The logarithm of profile shape parameter n versus central surface brightness μ_0. Sample and type coding the same as in Fig. 3.

indicator. There is indeed a strong correlation between the two Sérsic law parameters n and $\log r_0$ as well, which is shown for our sample in Fig. 7. Again we use $\log n$ instead of n as the independent quantity. The relation is certainly not linear. The best-fitting quadratic form is

$$\log r_0 = -4.502\,(\log n)^2 + 1.876\log n + 0.909\ , \qquad (10)$$

with an rms scatter in $\log r_0$ of $\sigma_{\rm logr} = 0.17$, which in terms of magnitudes (by multiplying with 5) corresponds to $\sigma_{\rm m}$ = 0.85 mag. This is comparable to the scatter of the $n - M$ relation (Fig. 3).

In contrast to the correlation with total magnitude (cf. above), there is no improvement by replacing $\log n$ with μ_0. This relation is shown in Fig. 8. The linear regression line is

$$\log r_0 = 0.264\,\mu_0 - 5.292\ , \qquad (11)$$

with a large $\sigma_{\rm logr}$ = 0.25, or $\sigma_{\rm m}$ = 1.25 mag. The scatter does not reduce by fitting a higher-order polynomial to the data.

One may wonder what a scatter around the mean $\log n - \log r_0$ relation of only $\sigma_{\rm logr}$ = 0.17 really means, in view of the much larger scatter in $\log r_0$ of $\sigma(\Delta \log r_0)$ = 0.40 for the difference between the growth curve fits and the differential fits, and likewise $\sigma(\Delta \log r_0)$ = 0.32 for the difference between our $\log r_0$ values and Durrell's (1997), as quoted in Sect. 2. Here, the surprising fact is that the scatter in $\log r_0$ is again only $\sigma_{\rm logr}$ = 0.17, albeit around a slightly different $\log n - \log r_0$ relation, if we switch to differential profile fitting. However, if n is determined from a growth curve fit and $\log r_0$ from a differential fit, or vice versa, this scatter turns out to be $\sigma_{\rm logr} \approx 0.3$. This we take as evidence that the best-fitting Sérsic parameters, for a given galaxy, are *not independent* from each other. We will elaborate on this important point further below.

Overall, then, the scatter in the Sérsic profile scaling relations – at least for our Virgo dwarf sample – is unacceptably large for use in the distance determination business. At least, these relations would make only rough & unreliable distance indicators. We have also looked for any dependence of the residuals on (1) the ellipticity of the dwarf galaxies, and (2) the distance to the center of the cluster, i.e. M87. No trend was found. There is no way how the scatter could be reduced to below $\simeq$ 0.7 mag. Thus the large scatter must essentially be *intrinsic – unless the Virgo cluster has a much greater depth than we thought*. This, in fact, is the claim of YC95. It will be rejected in the following section.

4. Critique of Young and Currie (1995)

Young & Currie's starting point (in YC94) was the $n - M$ relation for a sample of 26 Fornax cluster E and dE galaxies, for which they had derived Sérsic law parameters from Caldwell & Bothun's (1987) high-quality profiles. The scatter of this relation turned out to be a large $\sigma_{\rm m}$ = 0.88 mag. Only by the exclusion of four "outliers" was the scatter reduced to an encouragingly small $\sigma_{\rm m}$ = 0.47, and likewise to $\sigma_{\rm logr}$ = 0.108 for the $n - \log r$ relation (YC95). One could question this procedure, and one could criticize the obvious incompleteness of this Fornax cluster sample. But this is of no concern here. If the large scatter for Virgo cluster dwarfs is truly intrinsic, the usefulness, or reliability of these scaling relations as distance indicators is undermined at once – no matter what the reason for this difference between Fornax and Virgo is.

Our concern is Young & Currie's claim that the intrinsic scatter for Virgo dwarfs is as small as for Fornax dwarfs, which would mean that the large observed scatter for Virgo must be a *depth effect*. Such a claim can only be based on some *independent* information on the intrinsic scatter. YC95 apparently

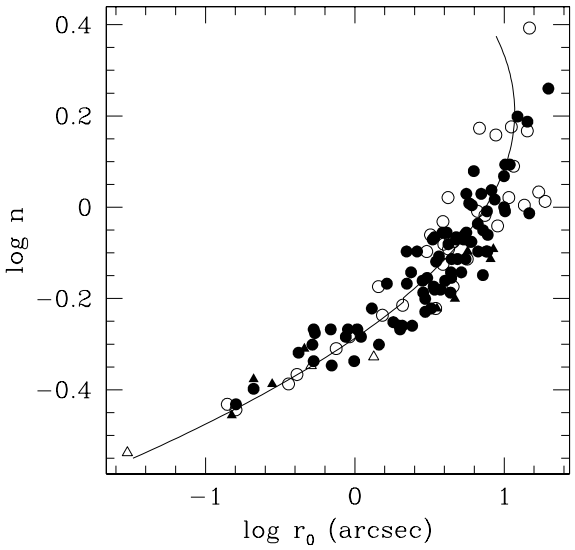

Fig. 7. The logarithm of shape parameter n versus the logarithm of Sérsic's radius scale r_0. Sample and type coding are the same as in Fig. 3. The line is the best-fitting $2^{\rm nd}$-order polynomial with $\log n$ as independent quantity, given by Eq. (10) in the text.

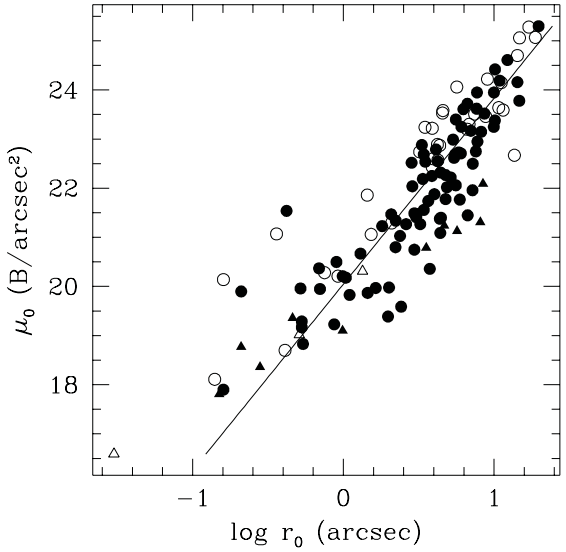

Fig. 8. Sérsic's central surface brightness μ_0 versus the logarithm of radius scale r_0. Sample and type coding are the same as in Fig. 3. The regression line is given by Eq. (11).

seized this information by applying both the $n - M$ and the $n - \log r$ relation *at the same time*.

Let us first see what happens if we do this with our own data. In Fig. 9 we have plotted the residuals from the $\log n - B_{\rm T}$ relation, calculated with respect to the regression line given by Eq. (6), *versus* $5\times$ the residuals from the $\log n - \log r_0$ relation, calculated with respect to the quadratic form given by Eq. (10). Obviously, the residuals are correlated. A formal regression for a fixed slope of 1, i.e.

$$\mathrm{res}(B_{\rm T} - \log n) = -5 \cdot \mathrm{res}(\log r_0 - \log n)\ , \qquad (12)$$

gives a scatter of $\sigma_{\rm m}$ = 0.86 mag, which is comparable to the values of $\sigma_{\rm m}$ = 0.92 (Fig. 3) and 0.85 mag (Fig. 7), respectively, for either relation *alone*. This must mean that the two relations, i.e. the parameters involved, are *not independent* – a suspicion spelled out already in the preceding section. The argument is quite simple: – *if* we would deal with two independent but equivalent "distance measurements" (in YC's terms), the scatter of the difference between the residuals, i.e. "distances" should equal the scatter of their sum, i.e. it should become *larger* than the scatter of a single relation by $\approx\sqrt{2}$ (assuming Poissonian statistics).

Such an interdependence should indeed be expected, as the three profile parameters of Sérsic's generalysed law are connected with total magnitude via Eq. (5): only three of the four quantities involved can be free. Our claim is that *the mean relation between* $\log n$ *and* μ_0 (Fig. 6) *is sufficient to cause the residual correlation* (Fig. 9). To prove this we have performed a simple Monte Carlo calculation.

The procedure was as follows: for the same dwarf sample we took the observed $B_{\rm T}$ and the best-fitting $\log n$ values. For every galaxy we then determined μ_0 from a Gaussian random distribution around the mean $\log n - \mu_0$ relation (Fig. 6) with σ_{μ_0} = 0.83 mag (note that both of these parameters are distance independent, hence the cluster depth cannot sneak in here). The forth parameter, $\log r_0$, is then fixed by Eq. (5), assuming perfect profile fits. Once all parameters are given, we fitted a quadratic form to the $\log n - \log r_0$ relation and finally determined the scatter of the relation between the $B_{\rm T} - \log n$ and $\log r_0 - \log n$ residuals, i.e. the scatter of the residual differences. This was repeated 10 000 times, after which everything was averaged. The average $\log n - \log r_0$ relation turned out to be very similar to the observed one, though with a somewhat larger scatter of $\sigma_{\rm logr}$ = 0.24 (versus 0.17 as observed), which corresponds to $\sigma_{\rm m}$ = 1.2 mag. Notwithstanding, the average scatter of the difference between res($B_{\rm T} - \log n$) and $-5 \cdot \mathrm{res}(\log r_0 - \log n)$ is again as low as σ = 0.85 mag (versus 0.86 as observed). For comparison, the scatter of their sum is 1.94 mag.

It is easy now to see what happens if this *intrinsic* connection between the $\log n - B_{\rm T}$ and $\log n - \log r_0$ relations is neglected: If we *assume* with Young & Currie (1995) that "... the $L - n$ and $R - n$ estimates are, to a good approximation, independent", we will *divide* $\sigma_{\rm m}$ = 0.86 mag from above by (at least)$\sqrt{2}$ and arrive at an "intrinsic" scatter of 0.61 mag for a single relation. Since this is significantly smaller than the 0.92 mag scatter of the $\log n - M$ relation, we are forced to Young & Currie's cluster depth interpretation, with $\sigma_{\rm depth} \approx$ 0.6 mag in this case, if we allow also for observational errors (cf. Sect. 3).

However, this does not yet explain why YC95 found a very small "intrinsic" scatter of 0.4 - 0.5 mag for their Virgo dwarfs. We think the reason for this additional effect must lie in the use of low-resolution (Schmidt) plates for surface photometry, where, e.g., the semi-stellar, central nuclei are smeared into the general profiles of the galaxies. In order to achieve a comparison with their high-resolution calibrating sample of Fornax cluster and Local Group dwarfs, YC95 had to convolve the profiles of the latter with a broad (FWHM $\approx 5''$) Gaussian, upon which

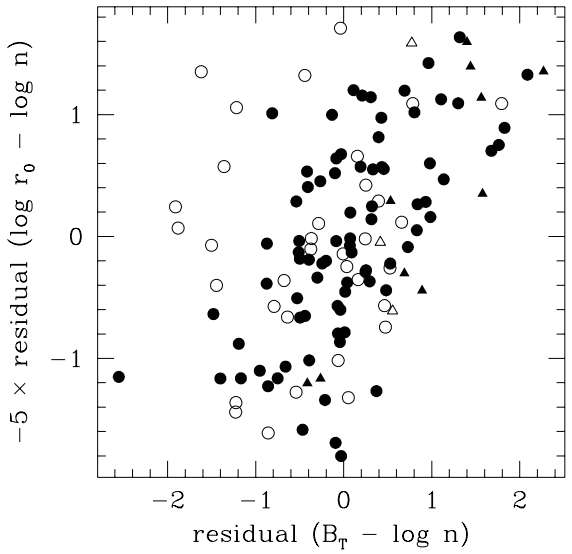

Fig. 9. Residual from the $\log n - B_{\rm T}$ relation [Eq. (6)] versus five times the residual from the $\log n - \log r_0$ relation [Eq. (10)]. The quantities plotted are magnitudes. Sample and type coding are the same as in Fig. 3.

the best-fitting Sérsic law parameters were determined. This was done for a whole grid of distance moduli of the calibrating galaxies. Then, for each individual Virgo dwarf a distance modulus was read from its locus with respect to the calibrating grid in the $n-M$ and $n-\log r$ plane, respectively. Finally, the comparison of the individual moduli as determined in both planes yielded the small "intrinsic" dispersion mentioned above. Here our suspicion is that *this small scatter merely mirrors the small scatter of the calibrating dwarfs*, having nothing to do with the Virgo sample. The convolution process changes the calibrating profiles *coherently* for both the $n-M$ and $n-\log r$ relations, such that the difference in distance for the Virgo dwarfs from these relations is bound to collapse to the intrinsic dispersion of the calibrating sample.

Whether our suspicion is correct could only be tested by a complete simulation of the analysis of YC95. However, as we have shown – based on the present data of superior quality – that the assumption of independence between the $n-M$ and $n-\log r$ relations is fundamentally flawed, there is no need for such a pursuit. In the absence of any independent evidence to the contrary, it is a principle of *conceptual economy* to assume that the large scatter of the Virgo sample is *intrinsic*, especially as long as there is no comparison sample (e.g., Fornax cluster) of similar completeness.

Having argued that there is no evidence that the large intrinsic scatter of Virgo sample is *not* intrinsic, we can also ask – Is there any positive evidence that it *is* intrinsic? We think the following simple test does provide such evidence.

Suppose the observed large scatter of the Virgo dwarfs *is* a depth effect, and the dwarfs are distributed in a prolate structure (rather than in a compact core as we thought) – pointing towards us (never mind!) and stretching from 8 to 20 Mpc in YC's distance scale (see Fig. 4 in YC95). Then these dwarfs (outside a cluster core) would have to possess rather small peculiar velocities, of order 50 k s^{-1} or less, and we would *expect to find a well-defined velocity-distance relation* for them, which should be the Hubble flow modulo a virgocentric infall pattern.

Fortunately, a fairly large subsample of 43 objects with known velocities out of our 128 Virgo dwarfs makes this test feasible. The velocities are listed in Table 1 (data from Binggeli et al. 1985, 1993). On the above assumption we now calculate pseudo distances for these 43 dwarfs from the residuals of the $\log n - B_{\rm T}$ relation:

$$D_{\rm pseudo} = 20 \cdot 10^{-0.2\,{\rm res}\,(B_{\rm T}-\log n)}\ [{\rm Mpc}]\ , \qquad (13)$$

where an average distance of 20 Mpc was chosen. It should be mentioned that in this case the regression line to which the residuals refer was calculated only for those 43 dwarfs; it is slightly, but not significantly different from Eq. (6).

In Fig. 10 we have plotted the resulting pseudo distances versus the heliocentric velocities for the 43 Virgo dEs with known redshifts. The same is shown in Fig. 11 for the better defined $\mu_0 - B_{\rm T}$ relation.

Obviously, our Virgo dwarfs do not follow a well-behaved velocity-distance relation. In the absence of any intrinsic scatter, all points should lie *within* the "infall boundary" indicated by the curved lines. These lines give the loci of galaxies that are falling into the cluster center along our line of sight (hence marking the *maximum* radial velocity). They are calculated with Kraan-Korteweg's (1986) infall model for a LG infall velocity of 220 k s^{-1}. Even with an intrinsic distance uncertainty of, say, 20 % (following YC95), i.e. $\sigma_{\rm D} \approx 4$ Mpc, or $\sigma_{\rm m} \approx 0.4$ mag, there are simply too many dwarfs (30 %) lying outside these boundaries to comply with Young & Currie's hypothesis.

Especially troublesome are the dwarfs with *negative* velocities. There are a number of them (5 out of < 100 with known redshifts), some of which have $v = -700$ k s^{-1} ! (cf. Binggeli et al. 1993). It is clear – for dynamical reasons – that these objects *must* lie in the core of the Virgo cluste.

It is, in fact, the mere *existence* of a small number of negative velocities among the dwarfs which provides the strongest (and most simple!) argument against the cluster depth hypothesis. For if these dwarfs are in the core (as admitted), their velocities most likely consitute the low-velocity tail of a broad (more or less Gaussian) velocity distribution. But this implies that for every dwarf with a negative velocity, there must be *many more* dwarfs – occupying the same spatial area, i.e. the cluster core – with a positive radial velocity. Hence, by a qualitative statistical argument, the *majority* of early-type Virgo dwarfs must certainly lie in the cluster core.

5. Conclusions

There is no evidence that the large scatter of the Sérsic profile parameter scaling relations for Virgo cluster dEs, in particular shape parameter n versus M or $\log r$, is other than intrinsic, i.e. being due to a (unexpectedly) large depth of the Virgo cluster. Young & Currie's (1995) claim to the contrary is based on low-resolution photometry and the untenable assumption that the

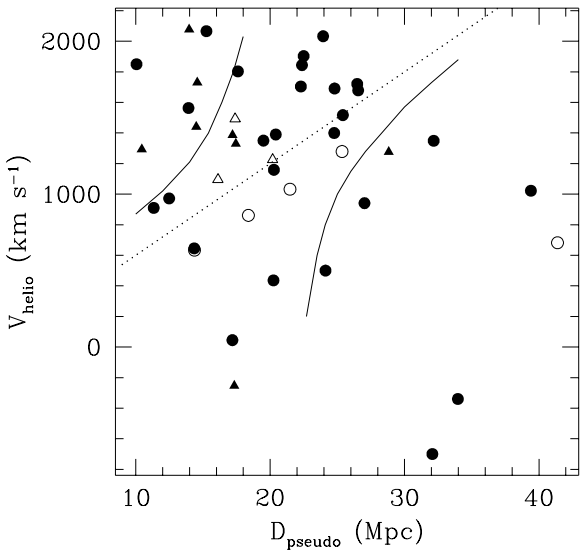

Fig. 10. Heliocentric velocity versus pseudo distance calculated from the $\log n - B_{\rm T}$ residual according to Eq. (13) for 43 Virgo dEs and dS0s with known redshifts. The type coding is the same as in Fig. 3. The dotted line corresponds to a quiet Hubble flow with H_0 = 60 km s^{-1} Mpc^{-1}. A galaxy falling through the cluster center (D = 20 Mpc, $\langle v \rangle$ = 1200 k s^{-1}) along our line of sight would move on one of the two curved lines. These are based on the virgocentric infall model of Kraan-Korteweg (1986) with a LG infall velocity of $v_{\rm LG}$ = 220 km s^{-1}.

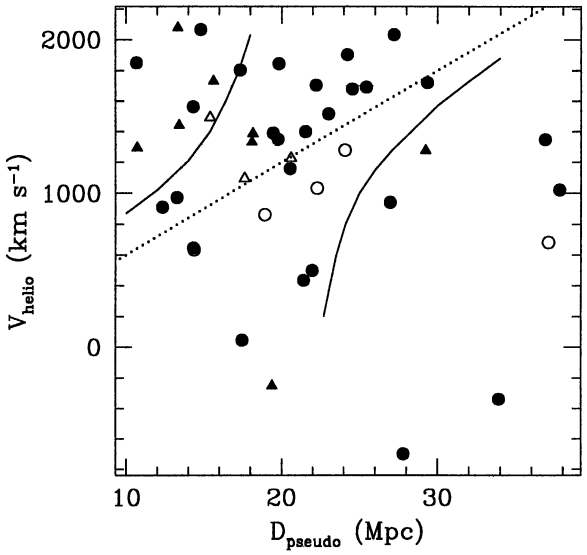

Fig. 11. The same as Fig. 10 but for the residuals of the $\mu_0 - B_{\rm T}$ relation [Fig. 5, Eq. (9)].

$n - M$ and $n - \log r$ relations are independent. On the other hand, there is some evidence in favour of a large intrinsic scatter by the absence of any correlation between the radial velocity and the residual from the $n - M$ relation for a sample of 43 Virgo dwarfs with known redshifts. Such a correlation would be expected if the $n - M$ residual were essentially a measure for the distance of a galaxy.

In consequence, we need not revise our view of the spatial distribution of dE galaxies and the morphology-density relation for dwarfs in general (e.g. Ferguson & Binggeli 1994). Dwarf ellipticals loosely distributed in a prolate cloud structure as put forward by YC95 would have been very difficult to understand, given that dEs are not known to exist (except as close companions) in the nearby "cloudy" field. The broad velocity distribution of Virgo cluster dEs, and the well-populated tail of negative velocity dwarfs in particular, is independent evidence that these galaxies are lying in the deep potential, i.e. in the narrow space of the core of the cluster. The filamentary distribution of Virgo spirals and irregulars (Fukugita et al. 1993, Yasuda et al. 1997), which was mentioned by YC95 as corroborative evidence, is an entirely different story. These types of galaxies are known to *avoid* the cluster core (Binggeli et al. 1987).

If the intrinsic dispersion of the $n - M$ or $n - \log r$ relation is much smaller for Fornax dwarfs than for Virgo dwarfs as it appears (which, however, might be caused by the incompleteness of YC's Fornax sample), we are in need of an explanation for this difference. In any case, the large intrinsic scatter for Virgo dwarfs is certainly not in favour of an application of the Sérsic profile scaling relations to distance measurements. These relations are very interesting and important in the context of the connection between E and dE (Jerjen & Binggeli 1997), but they can only be of limited use as distance indicators: the uncertainty in the distance modulus for a single galaxy cannot be reduced to below $\approx$ 0.7 mag. This is clearly inferior to the Tully-Fisher and $D_{\rm n} - \sigma$ methods (e.g. Jacoby et al. 1992), and it is no better than what can be achieved with the $\langle \mu \rangle_{\rm eff} - M$ relation for the same galaxies, which does not involve any profile fitting.

Acknowledgements. Financial support by the Swiss National Science Foundation is gratefully acknowledged. We thank Dr. J. van Gorkom for a crucial hint, and the referee, Dr. M.Fukugita, for his critical comments which helped to improve this paper.

References

Binggeli, B., Cameron, L. 1991, A&A, 252, 27 (= BC91)
Binggeli, B., Cameron, L. 1993, A&AS, 98, 297 (= BC93)
Binggeli, B., Popescu, C.C., Tammann, G.A. 1993, A&AS, 98, 275
Binggeli, B., Sandage, A., Tammann,G.A. 1985, AJ, 90, 1681
Binggeli, B., Tammann, G.A., Sandage, A. 1987, AJ, 94, 251
Caldwell, N., Bothun, G.D. 1987, AJ, 94, 1126
Caon, N., Capaccioli, M., D'Onofrio, M. 1993, MNRAS, 265, 1013
Davies, J.I., Phillipps, S., Cawson, M.G.M., Disney, M.J., Kibblewhite, E.J. 1988, MNRAS, 232, 239
de Vaucouleurs, G. 1948, Ann. d'Astrophys., 11, 247
D'Onofrio, M., Capaccioli, M., Caon, N. 1994, MNRAS, 271, 523
Durrell, P.R. 1997, AJ, 113, 531
Ferguson, H.C., Binggeli, B. 1994, A&AR, 6, 67
Fukugita, M., Okamura, S., Yasuda, N. 1993, ApJ, 412, L13
Jacoby, G.H., Branch, D., Ciardullo, R., Davies, R.L., Harris, W.E., Pierce, M.J., Pritchet, C.J., Tonry, J.L., Welch, D.L. 1992, PASP, 104, 599
Jerjen, H. 1995, PhD thesis, University of Basel
Jerjen, H., Binggeli, B. 1997, in: The Nature of Elliptical Galaxies, proceedings of the Second Stromlo Symposium, eds. M. Arnaboldi et al., ASP Conference Series 116, p. 239
King, I.R. 1966, AJ, 71, 64

Kraan-Korteweg, R.C. 1986, A&AS, 66, 255
Sérsic, J.-L. 1968, Atlas de galaxias australes, Observatorio Astronomico, Cordoba
Stein, P., Jerjen, H., Federspiel, M., 1997, A&A, 327, 952
Yasuda, N., Fukugita, M., Okamura, S. 1997, ApJS, 108, 417
Young, C.K., Currie, M.J. 1994, MNRAS, 268, L11 (= YC94)
Young, C.K., Currie, M.J. 1995, MNRAS, 273, 1141 (= YC95)